Inorganic Chemistry

Article

pubs.acs.org/IC

Synthesis, Characterization, and Reactivity of Ruthenium Hydride Complexes of N-Centered Triphosphine Ligands

Andreas Phanopoulos, Neil J. Brown, Andrew J. P. White, Nicholas J. Long,* and Philip W. Miller*

Department of Chemistry, Imperial College London, South Kensington, London SW7 2AZ, U.K.

Supporting Information

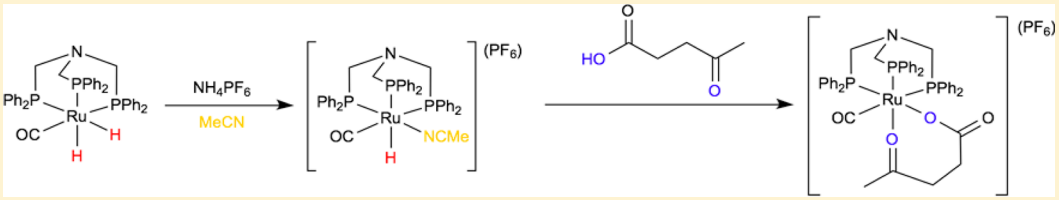

ABSTRACT: The reactivity of the novel tridentate phosphine ligand $N(CH_2PCyp_2)_3$ (N-triphos^{Cyp}, **2**; Cyp = cyclopentyl) with various ruthenium complexes was investigated and compared that of to the less sterically bulky and less electron donating phenyl derivative $N(CH_2PPh_2)_3$ (N-triphos^{Ph}, **1**). One of these complexes was subsequently investigated for reactivity toward levulinic acid, a potentially important biorenewable feedstock. Reaction of ligands **1** and **2** with the precursors $[Ru(COD)(methylallyl)_2]$ (COD = 1,5-cycloocatadiene) and $[RuH_2(PPh_3)_4]$ gave the tridentate coordination complexes $[Ru(tmm)\{N(CH_2PR_2)_3\text{-}\kappa^3P\}]$ (R = Ph (**3**), Cyp (**4**); tmm = trimethylenemethane) and $[RuH_2(PPh_3)\{N(CH_2PR_2)_3\text{-}\kappa^3P\}]$ (R = Ph (**5**), Cyp (**6**)), respectively. Ligands **1** and **2** displayed different reactivities with $[Ru_3(CO)_{12}]$. Ligand **1** gave the tridentate dicarbonyl complex $[Ru(CO)_2\{N(CH_2PPh_2)_3\text{-}\kappa^3P\}]$ (**7**), while **2** gave the bidentate, tricarbonyl $[Ru(CO)_3\{N(CH_2PCyp_2)_3\text{-}\kappa^2P\}]$ (**8**). This was attributed to the greater electron-donating characteristics of **2**, requiring further stabilization on coordination to the electron-rich Ru(0) center by more CO ligands. Complex **7** was activated via oxidation using AgOTf and O_2, giving the Ru(II) complexes $[Ru(CO)_2(OTf)\{N(CH_2PPh_2)_3\text{-}\kappa^3P\}](OTf)$ (**9**) and $[Ru(CO_3)(CO)\{N(CH_2PPh_2)_3\text{-}\kappa^3P\}]$ (**11**), respectively. Hydrogenation of these complexes under hydrogen pressures of 3−15 bar gave the monohydride and dihydride complexes $[RuH(CO)_2\{N(CH_2PPh_2)_3\text{-}\kappa^3P\}]$ (**10**) and $[RuH_2(CO)\{N(CH_2PPh_2)_3\text{-}\kappa^3P\}]$ (**12**), respectively. Complex **12** was found to be unreactive toward levulinic acid (LA) unless activated by reaction with NH_4PF_6 in acetonitrile, forming $[RuH(CO)(MeCN)\{N(CH_2PPh_2)_3\text{-}\kappa^3P\}](PF_6)$ (**13**), which reacted cleanly with LA to form $[Ru(CO)\{N(CH_2PPh_2)_3\text{-}\kappa^3P\}\{CH_3CO(CH_2)_2CO_2H\text{-}\kappa^2O\}](PF_6)$ (**14**). Complexes **3**, **5**, **7**, **8**, **11**, and **12** were characterized by single-crystal X-ray crystallography.

INTRODUCTION

The vast body of academic literature and industrially applied ruthenium-catalyzed reactions[1−9] is testament to the versatility and importance of ruthenium-based catalysts. The types of Ru catalytic transformations are diverse, varying from C−C cross-coupling reactions[10] and activation of inert C−H bonds[11] to the better-known metathesis[12] and hydrogenation reactions.[13] The majority of these ruthenium catalysts incorporate either mono- or bidentate phosphine ligands, which are ubiquitous in homogeneous catalysis owing to their highly tunable electronic and steric properties. Although less commonly used in catalytic applications than mono- or bidentate analogues, tridentate phosphines offer well-defined coordination geometries that can affect the stability of the catalytically active metal center, in some cases producing more active and robust catalysts. Consequently, tridentate ligands are receiving renewed academic and industrial interest for both coordination chemistry and catalysis.[14−16]

The most commonly studied tripodal phosphines are 1,1,1-tris(diphenylphosphinomethyl)ethane ($CH_3C(CH_2PPh_2)_3$, triphos^{Ph}) and its derivatives; these analogues mostly feature changes to the arm length between the apical carbon and phosphine or variance of the phosphine itself. Triphos-type ligands have been shown to coordinate to a wide range of early and late transition metals,[17−21] some of which have been evaluated for catalytic activity. Early examples include Rh-triphos^{Ph} complexes used for hydrogenation and hydroformylation of various alkenes[22] or the hydrogenation of quinoline, an important impurity found in fossil fuels that requires degradation.[23] More recently, Mo-triphos^{Ph} complexes were shown to coordinate and activate N_2, ultimately for conversion to ammonia or other high-value nitrogen-containing compounds,[24] while Ru-triphos complexes have been employed in formic acid dehydrogenation[25] and direct methylation of primary and secondary aromatic amines using carbon dioxide and molecular hydrogen.[26] Futhermore, Leitner et al. have reported the use of Ru-triphos^{Ph} systems in several highly desirable "green chemistry" reactions. A $[Ru(acac)_3]$/triphos system was used for the stepwise and tunable hydrogenation of two biomass-derived carboxylic acids (levulinic and itaconic acid) ultimately to 2- and 3-methyltetrahydrofuran, respec-

Received: January 8, 2014
Published: March 26, 2014

   dx.doi.org/10.1021/ic500030k | Inorg. Chem. 2014, 53, 3742−3752

tively; in both cases greater activity and scope was demonstrated over the use of analogous mono- or bidentate phosphine ligands.[27] This is significant, as methyltetrahydrofuran (MTHF) has been promoted as a greener ethereal solvent due to its production from renewable resources (such as corn starch), as well as its relative immiscibility with aqueous solutions in comparison to tetrahydrofuran (THF), facilitating workup and recovery.[28−30] A [Ru(COD)(methylallyl)$_2$]/triphos mixture was used for the selective hydrogenolysis via C−O bond cleavage of lignin model compounds, a vital step in the valorization process that aims to mildly depolymerize this natural product, while maintaining the desired functionality.[31] Finally, a preformed ruthenium complex, [Ru(tmm){$CH_3C(CH_2PPh_2)_3$-κ^3P}] (tmm = trimethylenemethane), was shown to give moderate turnover numbers for the hydrogenation of CO_2 to methanol,[32] a vital step for the recycling of carbon that may eventually lead to the realization of a sustainable carbon economy.

Despite the great interest in triphos complexes, the synthesis of triphos ligands is not always straightforward. Typically, highly air and moisture sensitive metal phosphide reagents are required that can result in low yields owing to incomplete substitution reactions. It would be desirable to obtain a more facile synthesis of triphos analogues that impart the same coordination chemistry features and catalytic activity. The previously reported N-centered triphos ligand *N,N,N*-tris(diphenylmethyl)amine, where the central bridgehead CH_3−C moiety in triphos^{Ph} is replaced by a single nitrogen atom to give $N(CH_2PPh_2)_3$ (N-triphos^{Ph}, **1**), is conveniently synthesized via a phosphorus variation of the Mannich reaction from the corresponding secondary phosphine.[33] Despite this facile synthesis, complexes with N-triphos ligands remain rare with only, to the best of our knowledge, a select few having been reported in the literature.[17,33−37] These ligands have previously been targeted within our group, as their facial coordination simplifies complexation by reducing the number of potential isomers, as well as resulting in a cis conformation of any other coordinated groups, facilitating reductive elimination during catalysis. It was for these primary reasons that *mer*-coordinating analogues were not investigated, despite many such ligands being studied for both complexation and catalysis.[38−40] Examples of such coordination geometries can be found in the vast body of work by Milstein et al., who have studied many pincer-type complexes, including the coordination and reactivity of PONOP ligands,[41] as well as CNN-, PNN-, and PNP-type ligands for activity toward hydrogenation of straight and cyclic esters,[42,43] and coupling reactions to form imines and pyrroles.[44,45] Other examples include POP- and PSP-type ligands that have similarly been investigated.[46,47]

Our previous investigations of N-triphos ligands have shown that steric encumberment of the phosphine arms determines whether a κ^3 or κ^2 coordination geometry is achieved.[17] Bulky phosphino-alkyl groups (dicyclohexyl- or di-*tert*-butylphosphine) only coordinate through two arms, while the third remains pendant; in addition, Gade et al. have recently shown that the smaller isopropyl derivative can bind through all three arms.[36] Since triphos complexes have previously been demonstrated to be highly effective catalysts, it would be of significant interest to expand the family of known κ^3-coordinating triphosphine ligands. Investigation into a wider range of sterically larger or smaller phosphines, in addition to exploring various phosphine substituents in order to tune electronic properties, may help elucidate critical aspects to improve catalytic activity. Herein, we report a series of new ruthenium N-triphos complexes, including three with the novel dicyclopentyl N-triphos ligand (N-triphos^{Cyp}, **2**). The coordination chemistry of **2** is compared to that of the less bulky phenyl derivative **1**, using three different ruthenium precursors. The reactivity of one of these complexes toward levulinic acid (LA) was assessed after initial activation by oxidation of the Ru(0) center, subsequent hydride formation under H_2 pressure, and a final activation step involving reaction with a proton donor.

RESULTS AND DISCUSSION

Ligand Synthesis. It has been previously shown by us that the coordination mode of N-triphos derivatives is controlled by the steric constraints imposed by the phosphine arms; consequently, the bulky di-*tert*-butyl and dicyclohexyl derivatives were found to exclusively form κ^2 coordination complexes, resulting in one free pendant arm.[17] The novel dicyclopentyl derivative N-triphos^{Cyp} (**2**) was therefore selected, as its reduction in steric bulk from the previously studied derivatives should enable the desired tridentate coordination. A switch to diarylphosphines was not explored, as dialkylphosphines possess the desired electron-donating ability required to adequately promote oxidative addition during catalytic cycles.

Ligand **1** was prepared as previously reported, via a conveniently air-stable phosphonium salt intermediate (Scheme 1a). Isolation and reaction of the phosphonium salt precursor for ligand **2** was found to give reduced yields; hence, ligand **2** was prepared via a one-pot in situ method (Scheme 1b).

Scheme 1. Synthesis of (a) N-triphos^{Ph} via a Phosphonium Salt Intermediate and (b) N-triphos^{Cyp} via a Dialkyl(hydroxymethyl)phosphine Intermediate

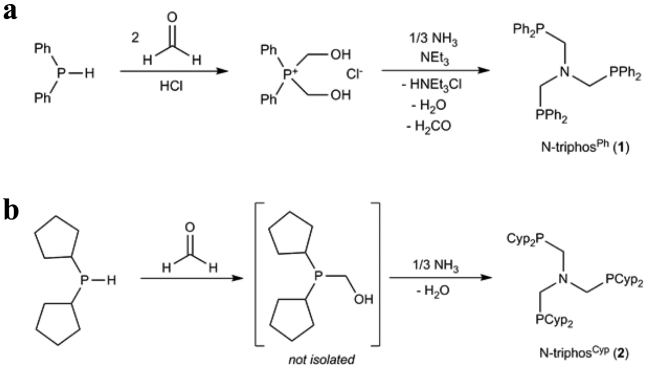

N-triphos^{Cyp} was prepared in moderate yield (59%) via the reaction of ammonia and in situ generated dicyclopentyl(hydroxymethyl)phosphine. Cooling the reaction mixture to −35 °C overnight resulted in the formation of a white crystalline solid that was isolated in high purity simply by filtration. The $^{31}P\{^1H\}$ NMR spectrum showed a single resonance at δ −18.4, and subsequent NMR spectra analysis revealed it does not exhibit strong J coupling between phosphorus and other spin-active nuclei. The reason for these unknown, however similar, spectral characteristics were observed for the ethyl, isopropyl, *tert*-butyl, and cyclohexyl derivatives, suggesting that this can be considered characteristic of this kind of ligand.[17,37,48]

Comparison of Coordination Chemistry between N-triphos^{Ph} and N-triphos^{Cyp}. Recent papers by the groups of

dx.doi.org/10.1021/ic500030k | Inorg. Chem. 2014, 53, 3742−3752

Scheme 2. Summary of N-triphos^{Ph} and N-triphos^{Cyp} Ru Complexes Prepared during This Study

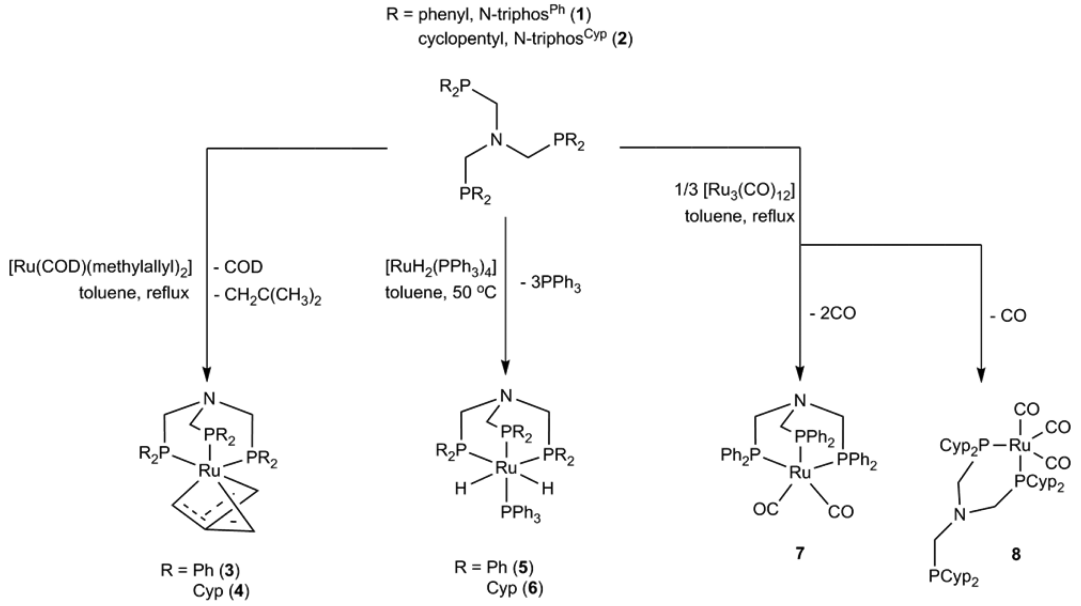

Leitner and Gade have shown [Ru(COD)(methylallyl)$_2$] to be a versatile starting material for producing κ^3 triphosphine ruthenium complexes.[31,36,37] When ligands **1** and **2** were reacted with 1 equiv of [Ru(COD)(methylallyl)$_2$] in toluene under reflux, all three phosphine arms were found to coordinate to the Ru center, displacing the COD ligand and one methylallyl moiety, generating facially capping κ^3 complexes (Scheme 2). Thus, ligands **1** and **2** afford the complexes [Ru(tmm){N(CH$_2$PPh$_2$)$_3$-κ^3*P*}] (**3**) and [Ru(tmm){N-(CH$_2$PPh$_2$)$_3$-κ^3*P*}] (**4**), respectively. The symmetric nature of complexes **3** and **4** is evident from the ^{31}P{^{1}H} NMR spectra, which each display singlets at δ 18.2 and 14.2, respectively. Similar to the compound [Ru(tmm){N(CH$_2$P^{i}Pr$_2$)$_3$-κ^3*P*}] reported by Gade et al.,[36] a singlet is observed for the signals assigned to the methylene protons of the tmm moieties in complex **4**, while the quaternary carbon (^{13}C{^{1}H} δ 102.8) is highly shifted, indicating η^4 coordination. Characterization of complex **3** by NMR proved difficult due to solubility issues, allowing only a weak ^{31}P{^{1}H} NMR spectrum to be recorded. High-resolution mass spectrometry (HRMS) showed only one peak cluster displaying the expected isotope pattern for ruthenium, strongly suggesting a monometallic structure. Additionally, crystals of **3** suitable for X-ray diffraction analysis were grown by allowing a dilute toluene solution to stand at room temperature for 5 days (Figure 1). The molecular structure revealed the complex has crystallographic C_3 symmetry about an axis that passes through N(1) and the ruthenium center, as well as confirming the expected distorted-octahedral structure. The short Ru−C^{tmm} distance observed (2.085 Å) also supports an η^4 coordination mode. Unlike complex **3**, the cyclopentyl derivative complex **4** is remarkably soluble in many solvents, and it is due to this, as well as its air and moisture sensitivity, that it was only possible to be isolated in relatively low yields (20%). Attempts to further extract or precipitate the desired complex invariably resulted in decomposition to "ruthenium black" and free ligand.

Reaction of ligands **1** and **2** in toluene at 50 °C with [Ru(H)$_2$(PPh$_3$)$_4$] results in ligand substitution of three PPh$_3$ units, resulting in the tridentate complexes [RuH$_2$(PPh$_3$){N-(CH$_2$PR$_2$)$_3$-κ^3*P*}] (R = phenyl (**5**), cyclopentyl (**6**)) (Scheme 2). Both complexes show a characteristic ^{31}P{^{1}H} NMR AM$_2$X splitting pattern, manifesting as two doublets of triplets and an apparent triplet. The two phosphine arms of the NP$_3$ ligands trans to the hydrides are easily identified from the relative 2:1 intensity in comparison to the other signals. The remaining two phosphorus signals were assigned on the basis of 2D ^{1}H/^{31}P{^{1}H} and ^{13}C{^{1}H}/^{31}P{^{1}H} NMR correlation experiments, indicating the remaining arms on the NP$_3$ ligands have δ_P values of 26.9 and 25.6 for complexes **5** and **6**, respectively.

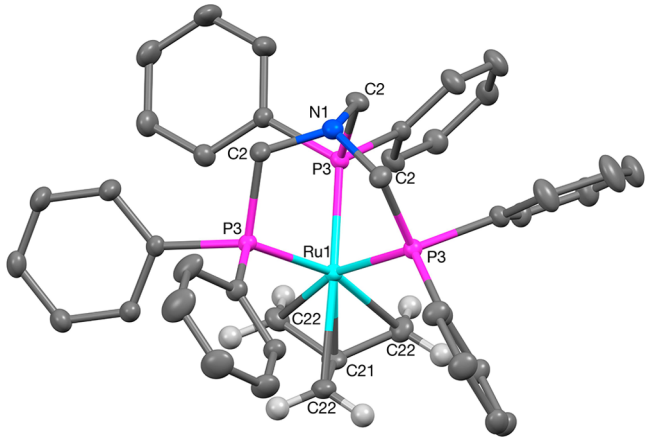

Figure 1. Crystal structure of the C_3-symmetric complex **3** (50% probability ellipsoids). Selected bond lengths (Å) and angles (deg) for **3**: Ru(1)−P(3), 2.2828(3); Ru(1)−C(21), 2.085(2); Ru(1)−C(22), 2.2518(13); P(3)−Ru(1)−C(21), 125.820(8); P(3)−Ru(1)−C(22), 103.89(4); P(3)−Ru(1)−P(3A), 89.211(12); P(3)−Ru(1)−C(22A), 164.01(4); P(3)−Ru(1)−P(3B), 89.211(12); P(3)−Ru−C(22B), 99.93(4); C(21)−Ru(1)−C(22), 38.51(4); C(21)−Ru(1)−P(3A), 125.820(8); C(21)−Ru(1)−C(22A), 38.51(4); C(21)−Ru(1)−P-(3B), 125.820(8); C(21)−Ru(1)−C(22B), 38.51(4); C(22)−Ru−P(3A), 99.93(4); C(22)−Ru(1)−C(22A), 65.26(6); C(22)−Ru(1)−P(3B), 164.01(4); C(22)−Ru(1)−C(22B), 65.26(6); P(3A)−Ru(1)−P(3B), 89.211(12); P(3A)−Ru(1)−C(22A), 103.89(4); P(3A)−Ru(1)−C(22B), 164.01(4); P(3B)−Ru(1)−C(22A), 99.93(4); P-(3B)−Ru(1)−C(22B), 103.89(4); C(22A)−Ru(1)−C(22B), 65.26(6).

dx.doi.org/10.1021/ic500030k | *Inorg. Chem.* 2014, 53, 3742−3752

The ^{1}H NMR spectra show distinctive hydride resonances that appear as complex multiplets centered around δ −7.73 and −9.72 for complexes **5** and **6**, respectively. When ^{1}H{^{31}P} spectra were recorded, these signals were found to simplify to singlets (Figure S7, Supporting Information). Crystals of **5** suitable for X-ray diffraction analysis were grown from a concentrated ether solution, and the structure shows a distorted-octahedral coordination geometry (Figure 2). Initially, synthesis of complex **5** was performed under reflux in diglyme; however, the inherent instability of the precursor $[RuH_2(PPh_3)_4]$ under these reaction conditions resulted in significantly lower yields. These lower yields were presumably due to a significant amount of decomposition occurring in tandem with product formation, as the precursor is highly fluxional in solution due to the disassociation/association of PPh_3. Changing the solvent to toluene and gently heating to 50 °C resulted in a yield increase from 19% to 54%.

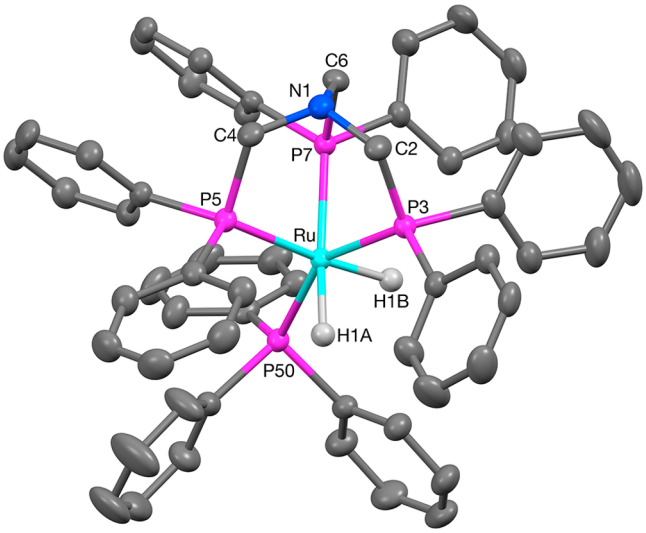

Figure 2. Crystal structure of **5** (50% probability ellipsoids). Selected bond lengths (Å) and angles (deg) for **5**: Ru−P(3), 2.2696(5); Ru−P(5), 2.3311(6); Ru−P(7), 2.3358(6); Ru−P(50), 2.3197(5); P(3)−Ru−P(5), 95.54(2); P(3)−Ru−P(7), 88.06(2); P(3)−Ru−P(50), 149.45(2); P(5)−Ru−P(7), 86.37(2); P(5)−Ru−P(50), 107.80(2); P(7)−Ru−P(50), 112.31(2).

$[Ru(CO)_2\{N(CH_2PPh_2)_3\text{-}\kappa^3P\}]$ (**7**), previously reported by us but not structurally characterized,[48] can be formed in high yields via the reaction of 3 equiv s of **1** with $[Ru_3(CO)_{12}]$ in toluene under reflux. The ^{31}P{^{1}H} NMR spectrum of **7** shows a single phosphorus resonance at δ 8.95 that remains unaltered when the temperature is lowered to −50 °C, demonstrating the highly fluxional nature of the complex in solution. X-ray diffraction analysis of crystals grown from a concentrated toluene solution show that, when crystalline, this complex adopts a distorted-square-pyramidal structure (for the square-based-pyramidal parameter τ of **7** see Table S2 in the Supporting Information) (Figure 3). Complex **7** is valuable as a precursor complex, from which a wide variety of potentially catalytically interesting complexes can be synthesized. It can be prepared in high yield and is a robust and stable complex that can be handled in air in the solid state, proving to be stable for days and only slowly oxidizing after several weeks to the carbonate complex $[Ru(CO_3)(CO)\{N(CH_2PPh_2)_3\text{-}\kappa^3P\}]$ (**11**). This transformation can be prevented by storing complex **7** under nitrogen.

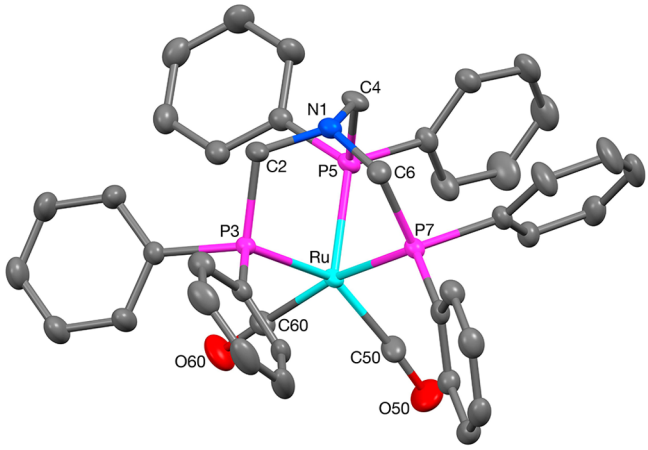

Figure 3. Crystal structure of **7** (50% probability ellipsoids). Selected bond lengths (Å) and angles (deg) for **7**: Ru−P(3), 2.3460(4); Ru−P(5), 2.3515(4); Ru−P(7), 2.3601(4); Ru−C(50), 1.8839(17); Ru−C(60), 1.8950(15); P(3)−Ru−P(5), 93.667(13); P(3)−Ru−P(7), 86.450(13); P(3)−Ru−C(50), 147.51(5); P(3)−Ru−C(60), 87.27(5); P(5)−Ru−P(7), 86.265(13); P(5)−Ru−C(50), 118.55(5); P(5)−Ru−C(60), 109.37(5); P(7)−Ru−C(50), 91.27(5); P(7)−Ru−C(60), 163.49(5); C(50)−Ru−C(60), 85.88(7).

Unlike $[Ru(COD)(methylallyl)_2]$ and $[RuH_2(PPh_3)_4]$, for which ligands **1** and **2** showed identical reactivity, reaction of 3 equiv of ligand **2** with $[Ru_3(CO)_{12}]$ in toluene under reflux overnight did not lead to tridentate coordination; instead, the κ^2 complex $[Ru(CO)_3\{N(CH_2PCyp_2)_3\text{-}\kappa^2P\}]$ (**8**) was formed. Crystals suitable for X-ray diffraction analysis were grown by layering a CH_2Cl_2 solution of **8** with methanol, confirming the bidentate coordination of **2**, which coordinates in a distorted-trigonal-bipyramidal geometry (Figure 4 and Table 1). The crystals of **8** were found to contain eight crystallographically independent complexes (**8-A**−**8-H**). Unsurprisingly, the N(1)···Ru separation seen in **8** is much larger (by ca. 0.46 Å) than those seen in the complexes with a tridentate N-triphos ligand (Table S3, Supporting Information). Neither sustained further heating to 165 °C in diglyme nor irradiation with a 400 W UV light resulted in ejection of a CO ligand and subsequent

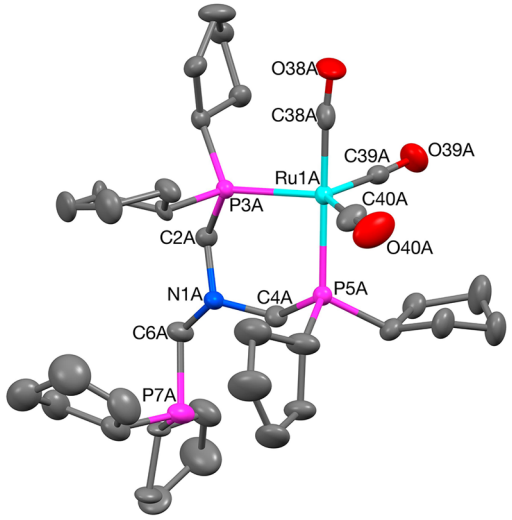

Figure 4. Structure of one (**8-A**) of the eight independent complexes present in the crystals of **8** (50% probability ellipsoids).

dx.doi.org/10.1021/ic500030k | Inorg. Chem. 2014, 53, 3742−3752

Table 1. Selected Bond Lengths (Å) for the Eight Independent Complexes (A−H) Present in the Crystals of 8

	Ru(1)−P(3)	Ru(1)−P(5)	Ru(1)−C(38)	Ru(1)−C(39)	Ru(1)−C(40)
A	2.3861(14)	2.3710(15)	1.902(6)	1.918(6)	1.904(6)
B	2.3669(14)	2.3778(15)	1.881(7)	1.899(6)	1.908(7)
C	2.3785(14)	2.3732(13)	1.895(6)	1.915(6)	1.894(6)
D	2.3800(14)	2.3837(14)	1.898(7)	1.907(7)	1.874(7)
E	2.3685(16)	2.3846(15)	1.895(6)	1.900(8)	1.904(8)
F	2.3672(14)	2.3866(14)	1.881(6)	1.907(7)	1.895(7)
G	2.3937(14)	2.3806(14)	1.904(6)	1.895(6)	1.915(7)
H	2.3591(14)	2.3845(14)	1.908(6)	1.912(6)	1.902(6)

Scheme 3. Activation of Complex 7 by Oxidation using Two Different Oxidants

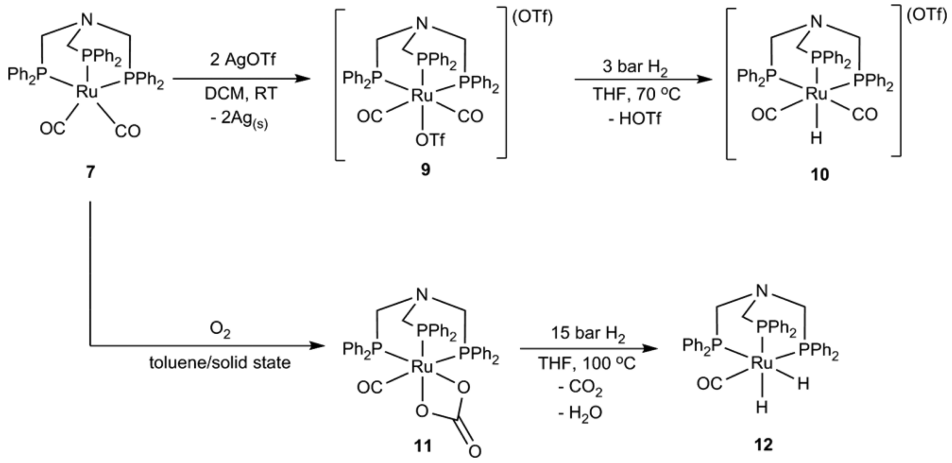

chelation of the pendant arm. Heating only resulted in decomposition of the complex into uncharacterizable products. Complex **8** remained completely unreactive under UV irradiation, with only starting material being observed, even after several hours, suggesting that the carbonyl ligands are highly stabilizing for the electron-rich ruthenium center. The increased electron-donating ability of the dicyclopentylphosphine arms (cf. diphenylphosphine) must require the ruthenium to be further stabilized by additional carbonyl ligands in comparison to the corresponding κ^3 N-triphos^{Ph} complex **7**.

Synthesis of Ruthenium Hydride Complexes from [Ru(CO)$_2${N(CH$_2$PPh$_2$)$_3$-κ^3*P*}] (7) and Subsequent Reactivity. In comparison to [Ru(CO)$_2$(PPh$_3$)$_3$], which forms the dihydride complex [RuH$_2$(CO)$_2$(PPh$_3$)$_2$] at room temperature under 1 bar of H_2,[49] complex **7** is unreactive toward molecular hydrogen even under forcing conditions of 50 bar and 100 °C. This is due to the added stability of the chelating NP_3 tridentate ligand and the reduced Ru(0) center, which is further stabilized by electron-withdrawing CO ligands. In order to produce a more reactive 16-electron complex, oxidation of **7** was undertaken using two different oxidizing agents (Scheme 3). Reaction of **7** with 2 equiv of AgOTf in CH_2Cl_2 at room temperature resulted in instant precipitation of metallic silver and the formation of [Ru(CO)$_2$(OTf){N(CH$_2$PPh$_2$)$_3$-κ^3*P*}](OTf) (**9**). The slow diffusion of diethyl ether into the CH_2Cl_2 solution gave a yellow crystalline precipitate that displayed a sharp doublet and triplet in the $^{31}P\{^1H\}$ NMR spectrum at δ −23.9 (2P) and 19.6 (1P), respectively. This implies that tridentate coordination of **1** persists; however, the complex is now six-coordinate with two different ancillary ligands. The presence of two distinct singlets in the $^{19}F\{^1H\}$ NMR spectrum at δ −76.8 and −78.5 indicates that one triflate is coordinating while the other is noncoordinating. This is also inferred from the FT-IR spectrum of **9**, which shows several very broad and intense peaks in the region 1158−1279 cm^{-1}, suggesting two different triflate environments. The presence of two carbonyl ligands is also evident from the FT-IR spectrum as two peaks at 2055 and 2095 cm^{-1}.

Reaction of **9** with molecular hydrogen at 3 bar for 18 h at 70 °C in THF led to high-yielding formation of the monohydride species [RuH(CO)$_2${N(CH$_2$PPh$_2$)$_3$-κ^3*P*}](OTf) (**10**) along with concomitant formation of 1 equiv of triflic acid. The $^{31}P\{^1H\}$ NMR spectrum of **10** still displays a doublet and triplet similar to those seen for complex **9**, while the $^{19}F\{^1H\}$ NMR spectrum, as expected, displays one resonance corresponding to the noncoordinating triflate anion. The ^1H NMR spectrum of **10** shows a characteristic doublet of triplets hydride signal centered at δ −6.75.

Oxidation of **7** using molecular oxygen (Scheme 3), by deliberate exposure of a solid sample to air for several weeks or by bubbling O_2 through a toluene solution of **7** for ca. 20 min, resulted in conversion to the carbonate complex [Ru(CO$_3$)(CO){N(CH$_2$PPh$_2$)$_3$-κ^3*P*}] (**11**). Reactivity similar to this has been observed for another ruthenium triphosphine complex using the *mer*-coordinating triphosphine PhP(CH$_2$CH$_2$CH$_2$PCy$_2$)$_2$.[50] The presence of the new carbonate ligand can clearly be observed in the FT-IR spectrum of **11**, which now displays only a single CO stretch at 1994 cm^{-1} and additional stretches typical of bidentate carbonate at 1565, 1434, 1272, and 1092 cm^{-1}.[51] Crystals suitable for X-ray diffraction analysis of complex **11** were grown by layering a concentrated CH_2Cl_2 solution with toluene and allowing this mixture to stand at room temperature overnight (Figure 5), confirming the bidentate coordination mode of carbonate. Similar to the crystal structures of **3** and **5**, **11** was found to

dx.doi.org/10.1021/ic500030k | Inorg. Chem. 2014, 53, 3742−3752

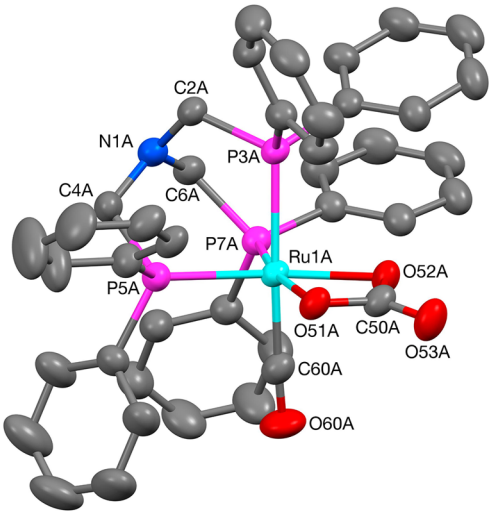

Figure 5. Structure of one (**11-A**) of the two independent complexes present in the crystals of **11** (50% probability ellipsoids).

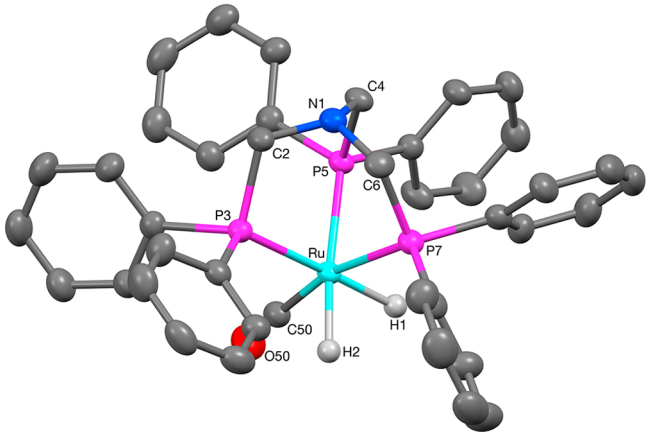

Figure 6. Crystal structure of **12** (50% probability ellipsoids). Selected bond lengths (Å) and angles (deg) for **12**: Ru−P(3), 2.3337(6); Ru−P(5), 2.3359(6); Ru−P(7), 2.3532(6); Ru−C(50), 1.881(3); P(3)−Ru−P(5), 88.95(2); P(3)−Ru−P(7), 90.48(2); P(3)−Ru−C(50), 99.99(8); P(5)−Ru−P(7), 88.36(2); P(5)−Ru−C(50), 99.47(8); P(7)−Ru−C(50), 166.97(8).

adopt a distorted-octahedral geometry and crystallized as two crystallographically independent complexes (**11-A** and **11-B**) (Table 2).

Reaction of **11** with a modest pressure of molecular hydrogen (3 bar) led to the formation of the neutral dihydride species $[Ru(H)_2(CO)\{N(CH_2PPh_2)_3\text{-}\kappa^3P\}]$ (**12**) within 18 h, though higher pressures (∼15 bar) gave complete conversion within 2 h; layering a concentrated toluene solution with methanol gave crystals suitable for X-ray diffraction analysis (Figure 6). Complex **12** shows an apparent doublet of doublets splitting pattern for the hydride resonance in the ^{1}H NMR spectrum, centered around δ −6.50, instead of the expected doublet of triplets due to phosphorus coupling. This same pattern was reported by Leitner et al. for the analogous Triphos^{Ph} complex $[RuH_2(CO)\{CH_3C(CH_2PPh_2)_3\text{-}\kappa^3P\}]$.[52] Complex **12** is reactive toward chlorinated solvents, instantly reacting with $CHCl_3$ and more slowly with CH_2Cl_2, forming three separate uncharacterized products, as is evident from 2D-^{31}P{^{1}H} NMR correlation experiments. The previously mentioned Triphos^{Ph} analogue has been implicated in several important catalytic cycles as a dormant form of the active catalytic species, hypothesized to be the cationic monohydride $[RuH\{CH_3C(CH_2PPh_2)_3\text{-}\kappa^3P\}]^+$,[52] including the hydrogenation of the biomass-derived levulinic and itaconic acids, as well as CO_2 reduction to methanol using hydrogen.[27,32]

The use of the air-stable carbonate complex **11** as a precursor for the synthesis of **12** and its analogues offers a route that is easier and milder than those previously reported for the equivalent Triphos-Ru dihydride complexes. These previous synthetic schemes require either harsh reaction conditions (120 bar of H_2, 150 °C, 20 h)[52] or several highly air-sensitive steps.[53,54] Since **11** is readily converted to **12** under pressures of hydrogen, **11** may be used as a stable precatalyst for hydrogenation reactions, as the dihydride complex **12** would form readily in situ before undergoing any necessary activation steps prior to catalysis.

Attempts to activate **8** by oxidation and facilitate tandem κ^3 coordination were not successful. Oxidation using O_2 did not give the analogous carbonate complex observed with **11** but instead led to decomposition and oxidation of the ligand. Presumably the pendant third arm reduces the overall stability of **8**, making it more susceptible to oxidative degradation processes.

The transformation of biomass-derived products into platform chemicals and solvents is of significant industrial interest, as these can offer green alternatives to products previously only accessible via petrochemical routes. The triphos complex $[RuH_2(CO)\{CH_3C(CH_2PPh_2)_3\text{-}\kappa^3P\}]$ has previously been reported as an active catalyst for the hydrogenation of biomass-derived acids, such as levulinic acid (LA), to industrial solvents.[27,52] The reactivity of the equivalent N-triphos complex **12** with LA was found to be markedly different from that of $[RuH_2(CO)\{CH_3C(CH_2PPh_2)_3\text{-}\kappa^3P\}]$. When 1 equiv of LA was treated with **12**, no reaction was found to occur in either nonpolar (C_6D_6) or polar (THF) solvents, even after heating under reflux overnight. In contrast, $[RuH_2(CO)\{CH_3C(CH_2PPh_2)_3\text{-}\kappa^3P\}]$ was reported to react cleanly with LA to form the coordinated complex $[RuH\{CH_3C(CH_2PPh_2)_3\text{-}\kappa^3P\}\{CH_3CO(CH_2)_2CO_2H\text{-}\kappa^2O\}]$, with concomitant release of H_2 and CO.[52] The lower reactivity of **12** toward LA can be overcome by initial in situ activation through formation of a monohydride cationic species by reaction with the proton donor NH_4PF_6, which has previously been shown to react with dihydride ruthenium complexes in this fashion.[55]

Table 2. Selected Bond Lengths (Å) for the Two Independent Complexes (A and B) Present in the Crystals of 11

	A	B		A	B
Ru(1)−P(3)	2.4018(7)	2.4188(7)	Ru(1)−O(51)	2.1303(19)	2.1265(19)
Ru(1)−P(5)	2.2985(7)	2.2872(8)	Ru(1)−O(52)	2.132(2)	2.124(2)
Ru(1)−P(7)	2.3007(7)	2.2986(7)	Ru(1)−C(60)	1.906(3)	1.905(3)
Ru(1)−C(50)	2.537(3)	2.537(3)			

dx.doi.org/10.1021/ic500030k | Inorg. Chem. 2014, 53, 3742−3752

Scheme 4. Reaction of 12 with NH_4PF_6 To Form 13 and Subsequent Coordination of Levulinic Acid To Form 14

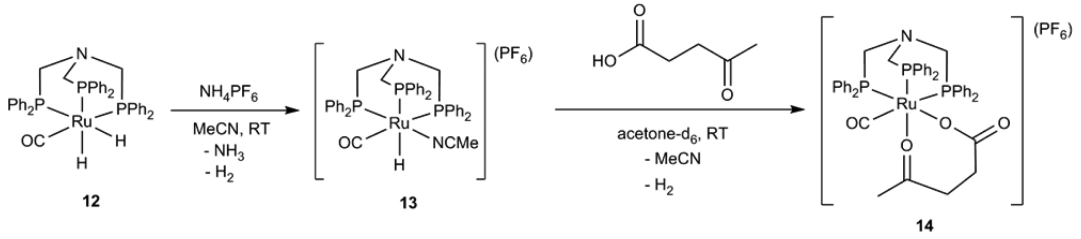

When **12** is reacted at room temperature with NH_4PF_6 in a coordinating solvent such as acetonitrile, it undergoes initial hydride loss as H_2, forming the reactive cationic 16-electron species $[RuH(CO)\{N(CH_2PPh_2)_3\text{-}\kappa^3P\}]^+$ that rapidly stabilizes through coordination of acetonitrile, forming $[RuH(CO)(MeCN)\{N(CH_2PPh_2)_3\text{-}\kappa^3P\}](PF_6)$ (**13**) (Scheme 4). This intermediate species is highly reactive and gives a $^{31}P\{^1H\}$ NMR spectrum that shows a multiplet and two doublets of doublets at δ −12.4, 3.9 ($^2J_{PP}$ = 31.6 Hz, $^2J_{PP}$ = 27.9) and 26.5 ($^2J_{PP}$ = 32.4 Hz, $^2J_{PP}$ = 22.3), respectively. The characteristic pseudo doublet of doublets in the hydride region of the ^1H NMR spectrum of **12** has now been replaced by a pseudo doublet of triplets for **13** at δ −6.3 ($^2J_{HP}$ = 77.5 Hz, $^2J_{HP}$ = 16.4 Hz).

The addition of 1.5 equiv of LA to a solution of **13** resulted in LA coordination to ruthenium through two oxygen donors via initial loss of hydride (as H_2) and the bound MeCN, forming $[Ru(CO)\{N(CH_2PPh_2)_3\text{-}\kappa^3P\}\{CH_3CO(CH_2)_2CO_2H\text{-}\kappa^2O\}](PF_6)$ (**14**) (Scheme 4). ^1H and $^{31}P\{^1H\}$ NMR spectra were recorded hourly for the reaction between **13** and LA at room temperature. The proton spectra showed the gradual disappearance of the Ru−H signal (Figure 7), while the phosphorus signals of **13** in the $^{31}P\{^1H\}$ NMR spectra also disappear and are replaced by a new pseudo triplet and doublet of **14** at δ −16.2 ($^2J_{PP}$ = 26.4 Hz) and 19.8 ($^2J_{PP}$ = 26.4 Hz), respectively (Figure 8). The apparent chemical equivalence of two phosphorus atoms arises from the similarity of the two coordinating oxygen atoms of LA trans to these phosphorus atoms, resulting in the observed apparent triplet and doublet instead of the expected three doublets of doublets signals. Continued NMR analysis revealed that the reaction is complete after 21 h.

The remarkable difference in reactivity between **12** and **13** with LA has implications for the use of these complexes as hydrogenation catalysts: namely, that **12** will *not* be an active catalyst for the hydrogenation of LA since the two components do not interact, presumably due to the high stability of **12**. Consequently, a proton source is necessary for the preactivation of this complex before LA can bind and subsequently undergo catalytic hydrogenation.

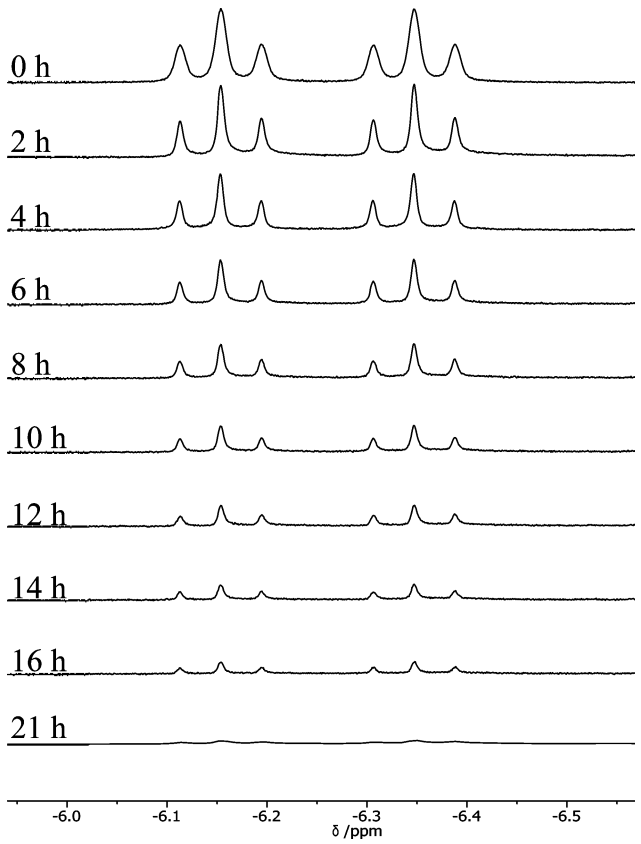

Figure 7. Stacked ^1H NMR spectra showing the hydride region for the conversion of **13** to **14**.

CONCLUSIONS

The coordination chemistry of the novel ligand $N(CH_2PCyp_2)_3$ (N-triphos^{Cyp}) was compared to that of the known N-$(CH_2PPh_2)_3$ (N-triphos^{Ph}) using three different ruthenium precursors. In two instances the analogous facially capping tridentate complexes were formed (complexes **3**−**6**). Reaction of ligands **1** and **2** with $[Ru_3(CO)_{12}]$ resulted in a less bulky phenyl derivative, forming the tridentate dicarbonyl species $[Ru(CO)_2\{N(CH_2PPh_2)_3\text{-}\kappa^3P\}]$ (**7**), while the more bulky cyclopentyl derivative exclusively gave the bidentate tricarbonyl species $[Ru(CO)_3\{N(CH_2PCyp_2)_3\text{-}\kappa^2P\}]$ (**8**).

Complex **7** was activated via oxidation using either AgOTf or oxygen, resulting in the formation of $[Ru(CO)_2(OTf)\{N(CH_2PPh_2)_3\text{-}\kappa^3P\}](OTf)$ (**9**) and $[Ru(CO_3)(CO)\{N(CH_2PPh_2)_3\text{-}\kappa^3P\}]$ (**11**). Subsequent hydrogenation of these complexes resulted in the facile formation of the ruthenium hydride complexes $[RuH(CO)_2\{N(CH_2PPh_2)_3\text{-}\kappa^3P\}](OTf)$ (**10**) and $[RuH_2(CO)\{N(CH_2PPh_2)_3\text{-}\kappa^3P\}]$ (**12**). The reactivity of **12** toward levulinic acid was investigated and found to coordinate only after an additional activation step with the proton donor NH_4PF_6 to give the solvent-bound $[RuH(CO)(MeCN)\{N(CH_2PPh_2)_3\text{-}\kappa^3P\}](PF_6)$ (**13**). This intermediary complex was found to react cleanly with levulinic acid via loss of hydride (as H_2) and acetonitrile. Levulinic acid then coordinates in a bidentate fashion through two oxygen donors, affording the cationic complex $[Ru(CO)\{N(CH_2PPh_2)_3\text{-}\kappa^3P\}\{CH_3CO(CH_2)_2CO_2H\text{-}\kappa^2O\}](PF_6)$ (**14**). Catalytic testing of complexes **3**−**12** is currently underway.

dx.doi.org/10.1021/ic500030k | Inorg. Chem. 2014, 53, 3742−3752

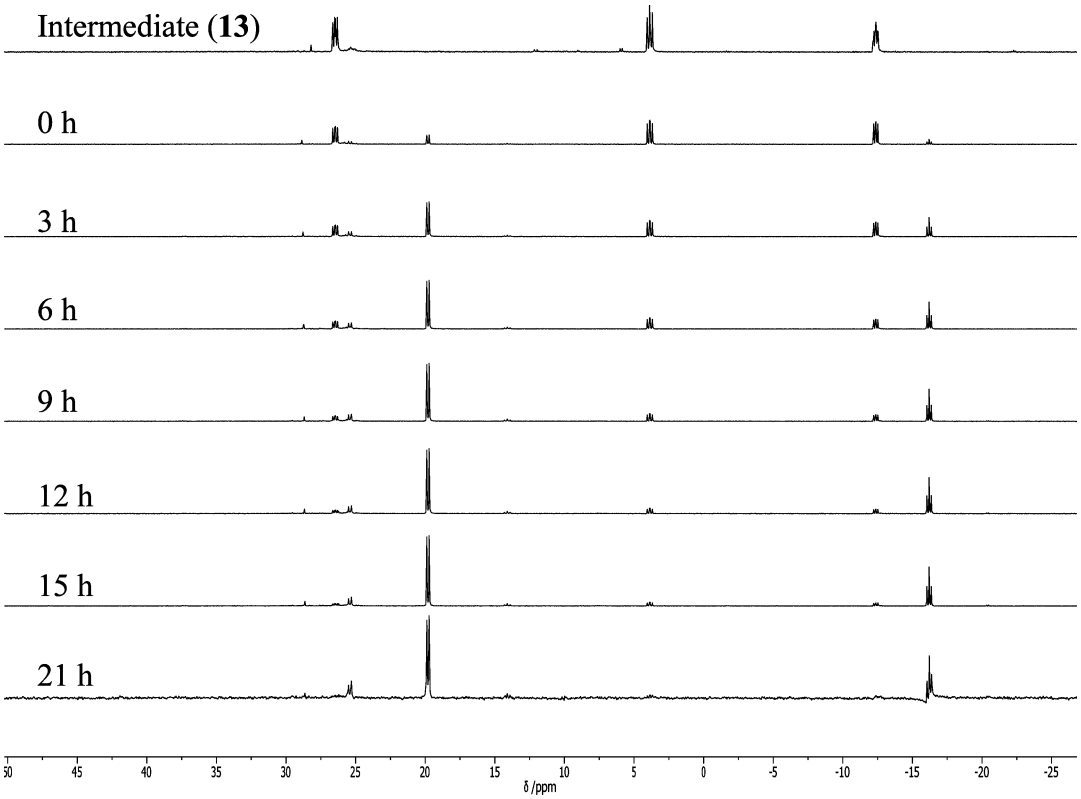

Figure 8. Stacked $^{31}P\{^{1}H\}$ NMR spectra showing the conversion of **13** to **14**.

EXPERIMENTAL SECTION

General Considerations. All preparations were carried out using standard Schlenk line techniques under an inert atmosphere of N_2 unless otherwise stated. Solvents were dried over standard drying agents and stored over 3 Å molecular sieves. All starting materials were of reagent grade purchased from either Sigma-Aldrich Chemical Co. or VWR International and used without further purification. Ligand **1** was prepared as previously reported.[33,48] ^{1}H, $^{13}C\{^{1}H\}$, and $^{31}P\{^{1}H\}$ NMR spectra were recorded on Bruker AV-400, AV-500, and DRX-400 spectrometers at 294 K unless otherwise stated. Chemical shifts are reported in ppm using the residual proton impurities in the solvents. Pseudo triplets and pseudo doublets of triplets that occur as a result of identical *J* value coupling to two or more chemically nonequivalent nuclei are assigned as dd, dt, or ddd and are recognized by the inclusion of only one or two *J* values. ^{13}C NMR spectra were assigned with the aid of DEPT-135, HSQC, and HMBC correlation experiments. Mass spectrometry analyses were conducted by the Mass Spectrometry Service, Imperial College London. Infrared spectra were recorded on a Perkin-Elmer Spectrum 100 FT-IR spectrometer. Elemental analyses were carried out by Mr. Stephen Boyer of the Department of Health and Human Science, London Metropolitan University. X-ray diffraction analysis was carried out by Dr. Andrew White of the Department of Chemistry at Imperial College. Details of the single-crystal X-ray diffraction analysis can be found in the Supporting Information.

Dicyclopentyl(hydroxymethyl)phosphonium Chloride. In a Schlenk flask were placed dicyclopentylphosphine (1.00 g, 5.87 mmol), degassed aqueous formaldehyde solution (35 wt %, 1.10 mL), and degassed concentrated HCl (37 wt %, 0.53 mL). The solution was stirred for 20 min at room temperature. Solvent was removed to give a viscous gum that was subsequently crystallized from acetone after being cooled to −5 °C to initiate crystallization. A white crystalline solid was obtained that was filtered while cold, washed with diethyl ether (3 × 2 mL), and dried in vacuo (683 mg, 2.56 mmol, 44%). ^{1}H NMR ($CDCl_3$, 400 MHz): δ 1.60−2.20 (m, 16H, CH_2^{Cyp}), 2.49−2.62 (m, 2H, CH^{Cyp}), 4.62 (s, 4H, PCH_2OH), 5.21 (br s, 2H, OH). $^{13}C\{^{1}H\}$ NMR ($CDCl_3$, 101 MHz): δ 26.0 (d, $^{2}J_{CP}$ = 9.6 Hz, CH_2^{Cyp}), 27.6 (s, CH_2^{Cyp}), 27.8 (d, $^{1}J_{CP}$ = 40.8 Hz, CH^{Cyp}), 51.2 (d, $^{1}J_{CP}$ = 54.0 Hz, PCH_2OH). $^{31}P\{^{1}H\}$ NMR ($CDCl_3$, 162 MHz): δ 31.8 (s). HRMS (ESI): *m*/*z* calcd for $C_{12}H_{24}O_2P$ ($[M - Cl]^+$) 231.1513, found 231.1509. Anal. Calcd for $C_{12}H_{24}O_2PCl$ (found): C, 54.03 (54.16); H, 9.07 (8.94).

***N,N,N*-Tris((dicyclopentylphosphino)methyl)amine (N-triphos^{Cyp}, 2).** *Method A.* In a Schlenk flask were placed dicyclopentylphosphine (1.00 g, 5.87 mmol) and methanol (5 mL). Degassed aqueous formaldehyde solution (35 wt %, 0.60 mL) was added, and the solution was stirred for 3 h at room temperature. A methanolic solution of NH_3 (2 M, 0.98 mL) was then added and the solution brought to reflux for 4 h, forming an opaque emulsion. The solution was placed in a freezer overnight, which resulted in the formation of a white crystalline precipitate (651 mg, 1.15 mmol, 59%). ^{1}H NMR (C_6D_6, 400 MHz): δ 1.42−2.09 (m, 54H, Cyp), 3.19 (s, 6H, NCH_2P). $^{13}C\{^{1}H\}$ NMR (C_6D_6, 101 MHz): δ 26.5 (d, $^{2}J_{CP}$ = 6.9 Hz, CH_2^{Cyp}), 26.8 (d, $^{2}J_{CP}$ = 7.0 Hz, CH_2^{Cyp}), 30.9 (d, $^{3}J_{CP}$ = 1.8 Hz, CH_2^{Cyp}), 31.0 (br s, CH_2^{Cyp}), 36.1 (d, $^{1}J_{CP}$ = 12.5 Hz, CH^{Cyp}), 58.4 (m, NCH_2P). $^{31}P\{^{1}H\}$ NMR (C_6D_6, 162 MHz): δ −18.5 (s). HRMS (ES): *m*/*z* calcd for $C_{33}H_{60}NP_3O_3$ ($[M + HO_3]^+$) 612.3864, found 612.3871. Anal. Calcd for $C_{33}H_{60}NP_3$ (found): C, 70.30 (70.25); H, 10.73 (10.67); N, 2.49 (2.54).

Method B. In a Schlenk flask were placed dicyclopentyl(hydroxymethyl)phosphonium chloride (626 mg, 2.35 mmol), NEt_3 (0.76 mL), and methanol (10 mL), and the solution was stirred for 10 min at room temperature. Subsequent addition of NH_3 (2 M, 0.39 mL) to the solution and stirring under reflux for 2 h resulted in an opaque emulsion, which when left in the freezer overnight allowed precipitation of the product as a white powder. The powder was washed with methanol (3 × 2 mL) and dried in vacuo to afford analytically pure **2** with characterization data identical with those produced via method A (98.9 mg, 0.175 mmol, 45%).

[Ru(tmm){N(CH_2PPh_2)$_3$-κ^3*P*}] (3). To a solution of **1** (357 mg, 0.584 mmol) in toluene (5 mL) was added [Ru(COD)(methylallyl)$_2$] (187 mg, 0.585 mmol), and the solution was stirred under reflux for 90 h. Within minutes the colorless solution turned yellow and

dx.doi.org/10.1021/ic500030k | *Inorg. Chem.* 2014, 53, 3742−3752

effervesence was observed. The product was observed to precipitate during the course of the reaction as an off-white powder that was highly insoluble in many solvents, hindering characterization and prohibiting collection of a $^{13}C\{^1H\}$ NMR spectrum. The precipitate was isolated via cannula filter, washed with toluene (3 × 3 mL), and dried in vacuo (259 mg, 0.338 mmol, 58%). Crystals suitable for X-ray diffraction analysis were grown from a dilute toluene solution at room temperature over 5 days. ^1H NMR (C_6D_6, 400 MHz, 353 K): δ 2.10 (s, 6H, CH_2^{tmm}), 3.92 (s, 6H, NCH_2P), 6.75−7.09 (m, 25H, Ph), 7.35−7.49 (m, 5H, Ph). $^{31}P\{^1H\}$ NMR (C_6D_6, 162 MHz, 353 K): δ 19.1 (s). HRMS (ES): m/z calcd for $C_{43}H_{43}NP_3{}^{102}Ru$ ($[M + H]^+$) 768.1652; found 768.1723. Anal. Calcd for $C_{43}H_{42}NP_3Ru$ (found): C, 67.35 (67.28); H, 5.52 (5.48); N, 1.83 (1.79).

[Ru(tmm){N(CH$_2$PCyp$_2$)$_3$-κ^3P}] (4). To a solution of **2** (89.2 mg, 0.158 mmol) in toluene (5 mL) was added [Ru(COD)(methylallyl)$_2$] (50.4 mg, 0.158 mmol), and the solution was stirred under reflux for 16 h. Cooling the solution to room temperature overnight resulted in the formation of orange crystals that were isolated via filtration, washed with methanol (3 × 2 mL), and dried in vacuo (22.3 mg, 0.0310 mmol, 20%). ^1H NMR ($CDCl_3$, 400 MHz): δ 1.23 (s, 6H, CH_2^{tmm}), 1.31−1.67 (m, 36H, CH_2^{Cyp}), 1.80−1.90 (m, 12H, CH_2^{Cyp}), 2.04−2.13 (m, 6H, CH^{Cyp}), 3.28 (s, 6H, NCH_2P). $^{13}C\{^1H\}$ NMR ($CDCl_3$, 101 MHz): δ 25.7−26.0 (m, CH_2^{Cyp}), 29.6 (s, CH_2^{Cyp}), 31.0 (s, CH_2^{Cyp}), 35.6−36.1 (m, CH_2^{tmm}), 46.6−46.7 (m, CH^{Cyp}), 51.2−51.6 (m, NCH_2P), 102.8 (s, C^{tmm}). $^{31}P\{^1H\}$ NMR ($CDCl_3$, 162 MHz): δ 14.2 (s). HRMS (ES): m/z calcd for $C_{37}H_{67}NP_3{}^{102}Ru$ ($[M + H]^+$) 720.3530, found 720.3569. Anal. Calcd for $C_{37}H_{66}NP_3Ru$ (found): C, 61.81 (61.76); H, 9.25 (9.30); N, 1.95 (1.89).

[Ru(H)$_2$(PPh$_3$){N(CH$_2$PPh$_2$)$_3$-κ^3P}] (5). To a solution of **1** (219 mg, 0.358 mmol) in toluene (10 mL) was added [RuH$_2$(PPh$_3$)$_4$] (412 mg, 0.358 mmol), the Schlenk flask was wrapped in silver foil, and the solution was stirred at room temperature for 1 h, before the temperature was raised to 50 °C and stirred for a further 11 h. The solvent was removed in vacuo and the yellow residue extracted with diethyl ether (3 × 5 mL). Concentrating the ether solution and allowing it to stand at room temperature overnight gave yellow crystals suitable for X-ray diffraction analysis (189 mg, 0.193 mmol, 54%). ^1H NMR (C_6D_6, 400 MHz): δ −7.73 (m, 2H, Ru−H), 3.93−4.10 (m, 6H, NCH_2P), 6.65−7.97 (m, 45H, Ph). $^{13}C\{^1H\}$ NMR (C_6D_6, 101 MHz): δ 52.8 (m, NCH_2P), 59.1 (m, NCH_2P), 127.2−128.0 (m, CH^{Ph}), 128.3 (d, J_{CP} = 6.6 Hz, CH^{Ph}), 132.2 (d, J_{CP} = 10.7 Hz, CH^{Ph}), 133.1 (t, J_{CP} = 5.6 Hz, CH^{Ph}), 133.9 (t, J_{CP} = 7.1 Hz, CH^{Ph}), 134.5 (d, J_{CP} = 11.2 Hz, CH^{Ph}), 142.0 (t, J_{CP} = 15.7 Hz, C^{Ph}), 143.2 (d, J_{CP} = 38.8 Hz, C^{Ph}), 144.6 (d, J_{CP} = 34.4 Hz, C^{Ph}). $^{31}P\{^1H\}$ NMR (C_6D_6, 162 MHz): δ 8.6 (dt, $^2J_{PP}$ = 25.9 Hz, 2P, P_{cis}), 27.3 (dt, $^2J_{PPh_3}$ = 210.8 Hz, $^2J_{PP}$ = 27.8 Hz, 1P, P_{trans}), 57.8 (dt, $^2J_{PPh_3P}$ = 210.0 Hz, $^2J_{PPh_3P}$ = 25.3 Hz, 1P, PPh_3). FT-IR (ν/cm^{-1}): hydride stretches 1915, 1882. HRMS (ES): m/z calcd for $C_{57}H_{52}NP_4{}^{102}Ru$ ($[M - H]^+$) 976.2094, found 976.2083. Anal. Calcd for $C_{57}H_{53}NP_4Ru$ (found): C, 70.07 (69.92); H, 5.47 (5.40); N, 1.43 (1.47).

[Ru(H)$_2$(PPh$_3$){N(CH$_2$PCyp$_2$)$_3$-κ^3P}] (6). To a solution of **2** (108 mg, 0.192 mmol) in toluene (10 mL) was added [RuH$_2$(PPh$_3$)$_4$] (221 mg, 0.192 mmol), and the solution was stirred at room temperature for 2 h before being heated to 50 °C for 14 h. The solvent was removed in vacuo, and the black-brown residue was washed with acetone (4 × 5 mL), forming an off-white/yellow powder that was dried in vacuo (61.5 mg, 66.2 μmol, 35%). ^1H NMR (C_6D_6, 500 MHz): δ −9.72 (m, 2H, Ru−H), 0.96−2.66 (m, 54H, Cyp), 3.24 (m, 4H, NCH_2P), 3.32 (br s, 2H, NCH_2P), 7.00 (dt, $^3J_{HH}$ = 7.4 Hz, $^5J_{HP}$ = 1.2 Hz, 3H, $CH^{para\text{-}Ph}$), 7.10−7.13 (dt, $^3J_{HH}$ = 7.9 Hz, $^3J_{PH}$ = 1.5 Hz, 6H, $CH^{ortho\text{-}Ph}$), 8.25−8.29 (m, 6H, $CH^{meta\text{-}Ph}$). $^{13}C\{^1H\}$ NMR (C_6D_6, 126 MHz): δ 25.0 (s, CH_2^{Cyp}), 26.1 (t, J_{CP} = 5.0 Hz, CH_2^{Cyp}), 26.2 (d, J_{CP} = 9.1 Hz, CH_2^{Cyp}), 26.8 (s, CH_2^{Cyp}), 26.9 (t, J_{CP} = 3.1 Hz, CH_2^{Cyp}), 27.5 (d, J_{CP} = 6.4 Hz, CH_2^{Cyp}), 28.7 (s, CH_2^{Cyp}), 29.4 (s, CH_2^{Cyp}), 29.6 (s, CH_2^{Cyp}), 29.9 (s, CH_2^{Cyp}), 30.7 (s, CH_2^{Cyp}), 31.0 (s, CH_2^{Cyp}), 51.0−51.1 (m, NCH_2P), 45.9 (d, $^1J_{CP}$ = 21.7 Hz, CH^{Cyp}), 47.3 (t, $^1J_{CP}$ = 8.7 Hz, CH^{Cyp}), 127.0 (d, $^3J_{CP}$ = 8.1 Hz, $CH^{meta\text{-}Ph}$), 127.5 (s, $CH^{para\text{-}Ph}$), 134.7 (d, $^2J_{CP}$ = 11.4 Hz, $CH^{ortho\text{-}Ph}$) 147.1 (d, $^1J_{CP}$ = 29.6 Hz C^{Ph}). $^{31}P\{^1H\}$ NMR (C_6D_6, 202 MHz): δ −5.3 (dt, $^2J_{PP}$ = 25.3 Hz, 2P, P_{cis}), 25.6 (dt, $^2J_{PPh_3}$ = 212.4 Hz, $^2J_{PP}$ = 28.2 Hz, 1P, P_{trans}), 61.9 (dt, $^2J_{PPh_3P}$ = 213.2 Hz, $^2J_{PPh_3P}$ = 22.9 Hz, 1P, PPh_3). FT-IR (ν/cm^{-1}): hydride stretches 1881, 1850. HRMS (ES): m/z found 394.1654 (85%), 751.2789 (60%). Anal. Calcd for $C_{51}H_{77}NP_4Ru$ (found): C, 65.92 (65.84); H, 8.35 (8.40); N, 1.51 (1.60).

Synthesis of [Ru(CO)$_2$(N(CH$_2$PPh$_2$)$_3$-κ^3P}] (7). This compound was previously reported.[48] It should be noted that the complex slowly reacts with $CDCl_3$ at room temperature. Crystals suitable for X-ray diffraction analysis were grown from a concentrated toluene solution left to stand at room temperature overnight.

[Ru(CO)$_3${N(CH$_2$PCyp$_2$)$_3$-κ^2P}] (8). To a solution of **2** (386 mg, 0.685 mmol) in toluene (15 mL) was added [Ru$_3$(CO)$_{12}$] (146 mg, 0.228 mmol), and the solution was stirred under reflux for 18 h, initially turning very dark before becoming lighter red. Removal of the solvent in vacuo and treatment of the resultant residue with methanol (10 mL) caused precipitation of an orange powder, which was isolated, washed with methanol (2 × 3 mL), and dried in vacuo. Dissolving the solid in dichloromethane (5 mL) and layering this solution with methanol (15 mL) and allowing it to stand at room temperature overnight afforded bright orange crystals suitable for X-ray diffraction experiments (241 mg, 0.322 mmol, 47%). ^1H NMR (C_6D_6, 400 MHz): δ 1.32−1.92 (m, 50H, CH^{Cyp} and CH_2^{Cyp}), 2.02−2.14 (m, 4H, CH^{Cyp}), 2.45 (s, 2H, NCH_2P), 2.66 (s, 4H, NCH_2P). ^{13}C NMR (C_6D_6, 101 MHz): δ 26.3 (m, CH_2^{Cyp}), 26.6 (t, J_{CP} = 4.6 Hz, CH_2^{Cyp}), 26.7 (d, J_{CP} = 6.5 Hz, CH_2^{Cyp}), 29.4 (br s, CH_2^{Cyp}), 30.7 (t, J_{CP} = 13.2 Hz, CH_2^{Cyp}), 35.7 (d, $^1J_{CP}$ = 12.2 Hz, CH^{Cyp}-bound phosphorus), 40.7 (t, $^1J_{CP}$ = 12.0 Hz, CH^{Cyp}-unbound phosphorus), 58.2 (dt, $^1J_{CP}$ = 17.0 Hz, $^3J_{CP}$ = 8.7 Hz, NCH_2P-unbound), 65.2 (q, $^1J_{CP}$ = 9.7 Hz, $^3J_{CP}$ = 7.6 Hz, NCH_2P-bound), 215 (t, $^2J_{CP}$ = 8.7 Hz, CO). ^{31}P NMR (C_6D_6, 162 MHz): δ −19.9 (s, 1P, unbound P), 29.0 (s, 2P, P−Ru). FT-IR (ν/cm^{-1}): carbonyl stretches 1867, 1902, 1978. HRMS (ES): m/z found 795.3019 (100%), 754.2841 (60%). Anal. Calcd for $C_{36}H_{60}NP_3O_3$ (found): C, 57.74 (57.81); H, 8.08 (7.98); N, 1.87 (1.95).

[Ru(CO)$_2$(OTf){N(CH$_2$PPh$_2$)$_3$-κ^3P}](OTf) (9). To a solution of **7** (124 mg, 0.162 mmol) in CH_2Cl_2 (5 mL) was added AgOTf (83.2 mg, 0.324 mmol), resulting in instantaneous precipitation of Ag(s). The resulting suspension was stirred for 1 h at room temperature. A pale yellow solution was filtered from the suspension via cannula, layered with diethyl ether (5 mL), and cooled to −20 °C overnight. A yellow microcrystalline powder was isolated, washed with diethyl ether (3 × 3 mL), and dried in vacuo overnight (110 mg, 0.103 mmol, 64%). ^1H NMR (CD_2Cl_2, 400 MHz): δ 4.57 (s, 2H, NCH_2P), 4.84 (app q, 4H, J_{HP} = 11.6 Hz, NCH_2P), 7.04−7.73 (m, 30H, Ph). $^{13}C\{^1H\}$ NMR (CD_2Cl_2, 101 MHz): δ 49.7 (td, $^1J_{CP}$ = 12.3 Hz, $^3J_{CP}$ = 5.7 Hz, NCH_2P^{cis}), 53.6 (dt, $^1J_{CP}$ = 17.4 Hz, $^3J_{CP}$ = 5.2 Hz, NCH_2P^{trans}), 119.1 (qd, $^1J_{CF}$ = 319.2 Hz, $^4J_{CP}$ = 2.38 Hz, bound CF_3), 121.5 (q, $^1J_{CF}$ = 319.3 Hz, unbound CF_3), 129.5 (t, J_{CP} = 5.1 Hz, C^{Ph}), 129.9 (d, J_{CP} = 10.9 Hz, C^{Ph}), 130.4 (t, J_{CP} = 5.1 Hz, C^{Ph}), 131.9 (m, C^{Ph}), 132.3 (d, J_{CP} = 9.5 Hz, C^{Ph}), 132.4 (s), 132.8 (d, J_{CP} = 2.5 Hz, C^{Ph}), 133.2 (d, J_{CP} = 4.5 Hz, C^{Ph}), 189.6 (m, CO). $^{31}P\{^1H\}$ NMR (CD_2Cl_2, 162 MHz): δ −23.9 (d, 2P, $^2J_{PP}$ = 19.5 Hz, P^{cis}), 19.6 (t, 1P, $^2J_{PP}$ = 19.5 Hz P^{trans}). $^{19}F\{^1H\}$ NMR (CD_2Cl_2, 376 MHz): δ −78.5 (br s, 3F, unbound CF_3), −76.8 (s, 3F, bound CF_3). FT-IR (ν/cm^{-1}): carbonyl stretches 2055, 2095; trifluoromethyl C−F stretches 1158 (br), 1203 (br), 1228 (br), 1279 (br); others 998, 1028, 1436. HRMS (ES): m/z calcd for $C_{42}H_{36}NP_3O_5SF_3{}^{102}Ru$ ($[M - OTf]^+$) 918.0523, found 918.0541. Anal. Calcd for $C_{43}H_{36}NP_3O_8S_2F_6Ru$ (found): C, 48.41 (48.54); H, 3.40 (3.35); N, 1.31 (1.29).

[RuH(CO)$_2${N(CH$_2$PPh$_2$)$_3$-κ^3P}](OTf) (10). A solution of **9** (65.0 mg, 60.9 μmol) in THF (5 mL) was placed under 3 bar of H_2 in a sealed ampule, heated to 70 °C, and stirred vigorously for 17 h, resulting in a color change from yellow to colorless. The solvent was removed in vacuo, and the resultant residue was washed with diethyl ether (4 × 5 mL), forming an off-white powder that was dried in vacuo overnight (39.8 mg, 0.0433 mmol, 71%). ^1H NMR (THF-d_8, 500 MHz): δ −6.75 (dt, 1H, $^2J_{HPcis}$ = 14.5 Hz, $^2J_{HPtrans}$ = 60.6 Hz, Ru−H), 4.45 (dd, 4H, $^2J_{HP}$ = 15.4 Hz, J = 71.6 Hz, NCH_2P), 4.89 (s, 2H, NCH_2P), 6.92−7.66 (m, 30H, Ph). $^{13}C\{^1H\}$ NMR (THF-d_8, 101 MHz): δ 51.2−51.6 (m, NCH_2P), 122.2 (q, J_{CF} = 320.4 Hz, CF_3),

dx.doi.org/10.1021/ic500030k | Inorg. Chem. 2014, 53, 3742−3752

129.6 (t, J_{CP} = 4.8 Hz, CH^{Ph}), 130.2 (d, J_{CP} = 10.1 Hz, CH^{Ph}), 131.1 (d, J_{CP} = 12.7 Hz, CH^{Ph}), 132.5 (t, J_{CP} = 5.0 Hz, CH^{Ph}), 132.8 (d, J_{CP} = 11.3 Hz, CH^{Ph}), 133.9 (t, J_{CP} = 5.0 Hz, CH^{Ph}), 134.8 (d, J_{CP} = 21.7 Hz, C^{Ph}), 136.8 (d, J_{CP} = 36.6 Hz, C^{Ph}), 197.3−198.3 (m, CO). $^{31}P\{^1H\}$ NMR (THF-d_8, 162 MHz): δ −16.8 (t, 1P, $^2J_{PP}$ = 25.5 Hz, P^{trans}), −2.01 (d, 2P, $^2J_{PP}$ = 25.5 Hz, P^{cis}). ^{19}F NMR (THF-d_8, 470 MHz): δ −79.2 (s). FT-IR (ν/cm^{-1}): carbonyl stretches 2004, 2051; trifluoromethyl C−F stretches 1025 (br), 1090 (br), 1156 (br), 1224 (br), 1259 (br); others 1435, 1485. HRMS (ES): m/z calcd for $C_{41}H_{37}NP_3O_2S^{102}Ru$ ($[M - OTf]^+$) 770.1081, found 770.1094. Anal. Calcd for $C_{43}H_{36}NP_3O_8S_2F_6Ru$ (found): C, 54.90 (54.81); H, 4.06 (4.12); N, 1.52 (1.62).

[Ru(CO$_3$)(CO){N(CH$_2$PPh$_2$)$_3$-κ^3*P*}] (11). *Method A.* A partially dissolved suspension of **7** (280 mg, 0.364 mmol) in toluene (5 mL) was bubbled with O_2 for 10−15 min. The orange precipitate that formed was collected by filtration, washed with toluene (2 × 3 mL) and diethyl ether (2 × 3 mL), and dried in vacuo (204 mg, 0.255 mmol, 70%). Crystals suitable for X-ray diffraction analysis were grown by layering a concentrated dichloromethane solution of **11** with toluene. ^1H NMR ($CDCl_3$, 400 MHz): δ 4.05−4.17 (m, 6H, NCH_2P), 6.92−7.72 (m, 30H, Ph). $^{13}C\{^1H\}$ NMR ($CDCl_3$, 101 MHz): δ 50.1 (dt, $^1J_{CP}$ = 18.5 Hz, $^3J_{CP}$ = 6.2 Hz, NCH_2P^{trans}), 51.1 (td, $^1J_{CP}$ = 12.5 Hz, $^3J_{CP}$ = 3.2 Hz, NCH_2P^{cis}), 128.2 (d, J_{CP} = 6.8 Hz, CH^{Ph}), 128.5−128.7 (m, CH^{Ph}), 129.4 (br s, CH^{Ph}), 129.8 (s, CH^{Ph}), 130.1 (s, CH^{Ph}), 130.9 (t, J_{CP} = 5.0 Hz, CH^{Ph}), 132.5 (d, J_{CP} = 9.3 Hz, CH^{Ph}), 132.8 (t, J_{CP} = 4.9 Hz, CH^{Ph}), 133.3−134.0 (m, C^{Ph}), 136.2−136.9 (m, C^{Ph}), 167.8 (s, CO_3), 194.0 (dt, $^2J_{CPtrans}$ = 106.4 Hz, $2J_{CPcis}$ = 11.0 Hz, CO). $^{31}P\{^1H\}$ NMR ($CDCl_3$, 162 MHz): δ −23.5 (t, $^2J_{PP}$ = 33.8 Hz, P^{cis}), 15.9 (d, $^2J_{PP}$ = 33.3 Hz, P^{trans}). FT-IR (ν/cm^{-1}): carbonyl stretch 1994; κ^2-carbonate stretches 1565, 1434; κ^2-carbonate bends 1272, 1092; others 1485. HRMS (ES): m/z calcd for $C_{41}H_{37}NP_3O_4{}^{102}Ru$ ($[M + H]^+$) 802.0979, found 802.1005. Anal. Calcd for $C_{41}H_{36}NP_3O_4Ru$ (found): C, 61.50 (61.27); H, 4.53 (4.34); N, 1.75 (1.84).

Method B. A sample of **7** (63.4 mg, 0.0825 mmol) was deliberately exposed to air for 5 weeks. Washing with wet toluene (5 × 1 mL) and wet diethyl ether (5 × 1 mL) and drying in air afforded a yellow-brown powder with characterization data identical with those produced via method A (48.0 mg, 59.9 μmol, 73%).

[Ru(H)$_2$(CO){N(CH$_2$PPh$_2$)$_3$-κ^3*P*}] (12). A solution of **11** (763 mg, 0.953 mmol) in THF (25 mL) was injected into a high-pressure reactor under a flow of nitrogen. The atmosphere was changed to hydrogen and pressurized to 15 bar at room temperature before the mixture was heated to 100 °C (increasing the internal pressure to ca. 20 bar) and stirred for 2 h. After the mixture was cooled to room temperature, the gas was carefully vented and the atmosphere changed to nitrogen. The solution was transferred from the reactor to a Schlenk flask, filtered, and diluted with methanol (20 mL), and the solvent was removed in vacuo, giving an orange powder that was washed with methanol (3 × 5 mL) and diethyl ether (3 × 5 mL) and dried in vacuo (365 mg, 0.492 mmol, 52%). Crystals suitable for X-ray diffraction analysis were grown from a concentrated toluene solution layered with methanol. ^1H NMR (C_6D_6, 400 MHz): δ −6.50 (dd, 2H, $^2J_{HPtrans}$ = 49.3 Hz, $^2J_{HPcis}$ = 18.8 Hz, Ru−H), 3.66 (s, 2H, NCH_2P), 3.82 (m, 4H, NCH_2P), three multiplets 6.69−6.87, 7.27−7.34 and 7.51−7.61 (m, 30H, Ph). $^{13}C\{^1H\}$ NMR (C_6D_6, 101 MHz): δ 51.8 (m, NCH_2P), 53.5 (m, NCH_2P), 127.7−128.3 (m, CH^{Ph}), 128.5 (d, J_{CP} = 11.2 Hz, CH^{Ph}), 131.8 (t, J_{CP} = 6.2 Hz, CH^{Ph}), 132.5 (d, J_{CP} = 12.0 Hz, CH^{Ph}), 132.9 (t, J_{CP} = 6.9 Hz, CH^{Ph}), 138.6 (dt, J_{CP} = 38.8 Hz, J_{CP} = 3.5 Hz, C^{Ph}), 139.6 (m, C^{Ph}) 141.0 (m, C^{Ph}), 209.2 (dt, $^2J_{CPtrans}$ = 73.7 Hz, $^2J_{CPcis}$ = 8.3, CO). $^{31}P\{^1H\}$ NMR (C_6D_6, 162 MHz): δ 8.5 (d, $^2J_{PP}$ = 35.7 Hz, 2P), 18.8 (t, $^2J_{PP}$ = 34.8 Hz, 1P). FT-IR (ν/cm^{-1}): Ru−CO and Ru−H stretches 1858, 1926, 2190. MS (ES) m/z calcd for $C_{40}H_{38}NP_3O^{102}RuK$ ($[M + K]^+$) 782.1, found 783.1. Anal. Calcd for $C_{40}H_{38}NP_3ORu$ (found): C, 64.68 (64.50); H, 5.16 (4.97); N, 1.89 (1.73).

NMR-Scale Reaction of [RuH$_2$(CO){N(CH$_2$PPh$_2$)$_3$-κ^3*P*}] (12), NH$_4$PF$_6$, and Levulinic Acid. A solution of **12** (48.4 mg, 65.2 μmol) in toluene (2 mL) was added via cannula to a stirred solution of NH_4PF_6 (10.6 mg, 65.0 μmol) in acetonitrile (2 mL), and the cannula was washed through with additional acetonitrile (2 × 2 mL). The solution was stirred at room temperature for 2 h, before the solvent was removed in vacuo, affording the intermediate [RuH(CO)-(MeCN)N(CH$_2$PPh$_2$)$_3$-κ^3*P*}] (**13**) as a brown powder that was washed with hexane (3 × 3 mL) and dried in vacuo for 30 min. Intermediate **13** was dissolved in degassed acetone-d_6 (0.5 mL), and initial ^1H and $^{31}P\{^1H\}$ NMR spectra were recorded. ^1H NMR (400 MHz, acetone-d_6): δ −6.30 (ddd, 1H, $^2J_{HP}$ = 77.5 Hz, $^2J_{HP}$ = 16.4 Hz, Ru−H). $^{31}P\{^1H\}$ NMR (162 MHz, acetone-d_6): δ −144.2 (septet, 1P, $^1J_{PF}$ = 708.4 Hz, PF_6^-), −12.4 (m), 3.9 (dd, 1P, $^2J_{PP}$ = 31.6 Hz, $^2J_{PP}$ = 27.5 Hz), 26.5 (dd, 1P, $^2J_{PP}$ = 32.4 Hz, $^2J_{PP}$ = 22.3 Hz). In the NMR tube was placed a solution of levulinic acid (10.8 mg, 93.0 μmol, 1.43 equiv) in degassed acetone-d_6 (0.5 mL), and the solution was stirred for 2 min using a vortex stirrer. ^1H and $^{31}P\{^1H\}$ NMR spectra were recorded every 1 h for 16 h, with the first being taken approximately 10 min after stirring. The reaction was complete within 21 h. ^1H NMR (400 MHz, acetone-d_6): δ 2.23 (s, 3H, CH_3^{LA}), 2.67 (t, 2H, $^3J_{HH}$ = 5.8 Hz, CH_2^{LA}), 2.84 (t, 2H, $^3J_{HH}$ = 5.9 Hz, CH_2^{LA}), 4.55−4.68 (m, 6H, NCH_2P), 6.95−7.68 (m, 30H, Ph). $^{13}C\{^1H\}$ NMR (101 MHz, acetone-d_6): δ 28.1 (s, CH_3^{LA}), 37.5 (CH_2^{LA}), 38.2 (s, CH_2^{LA}), 50.7 (td, $^1J_{CP}$ = 13.2 Hz, $^3J_{CP}$ = 5.4 Hz, NCH_2P), 51.7 (dt, $^1J_{CP}$ = 19.1 Hz, $^3J_{CP}$ = 5.4 Hz, NCH_2P), 129.1 (d, J_{CP} = 9.6 Hz, CH^{Ph}), 131.0 (d, J_{CP} = 2.6, CH^{Ph}), 131.6 (s, CH^{Ph}), 131.9 (s, CH^{Ph}), 132.0 (t, J_{CP} = 5.1 Hz, CH^{Ph}), 133.2 (t, J_{CP} = 4.6 Hz, CH^{Ph}), 133.7 (d, J_{CP} = 9.5 Hz, CH^{Ph}), 174.0 (s, CO^{LA}), 192.0 (s, CO^{LA}), 206.7 (d, J_{CP} = 3.0 Hz, CO). $^{31}P\{^1H\}$ NMR (162 MHz, acetone-d_6): δ −16.2 (dd, $^2J_{PP}$ = 26.4 Hz, P^{trans}), 19.8 (dd, $^2J_{PP}$ = 26.4 Hz, P^{cis}). MS (ES): m/z calcd for $C_{45}H_{43}NP_3O_4{}^{102}Ru$ ($[M - PF_6]^+$) 856.1, found 856.4.

■ ASSOCIATED CONTENT

Ⓢ Supporting Information

Figures, tables, and CIF files giving $^{31}P\{^1H\}$ NMR spectra of ligand **2**, complexes **3**−**12**, and intermediate **13**, a comparison of the hydride region of ^1H and $^1H\{^{31}P\}$ NMR spectra of **5** and **6**, and additional crystallographic data, including 50% probability ellipsoid ORTEP diagrams of all independent crystal structures. This material is available free of charge via the Internet at http://pubs.acs.org.

■ AUTHOR INFORMATION

Corresponding Authors

*E-mail for N.J.L.: n.long@imperial.ac.uk.

*E-mail for P.W.M.: philip.miller@imperial.ac.uk.

Author Contributions

The manuscript was written through contributions of all authors. All authors have given approval to the final version of the manuscript. N.J.B. assissted in setting up the high-pressure reactor and initial hydrogenation reactions. A.J.P.W. was primarily responsible for the X-ray crystallographic analysis.

Notes

The authors declare no competing financial interest.

■ ACKNOWLEDGMENTS

We thank Imperial College London for funding, via the Frankland Chair endowment. Johnson Matthey plc are also thanked for the loan of the precious-metal salts used in this work.

■ REFERENCES

(1) Bruneau, C.; Dixneuf, P. H. *Ruthenium Catalysis and Fine Chemicals*; Springer: New York, 2004.

(2) Naota, T.; Takaya, H.; Murahashi, S.-I. *Chem. Rev.* **1998**, *98*, 2599−2660.

(3) Arockaim, P. B.; Bruneau, C.; Dixneuf, P. H. *Chem. Rev.* **2012**, *112*, 5879−5918.

(4) Trost, B. M.; Toste, F. D.; Pinkerton, A. B. *Chem. Rev.* **2001**, *101*, 2067−2096.
(5) Vougioukalakis, G. C.; Grubbs, R. H. *Chem. Rev.* **2010**, *110*, 1746−1787.
(6) Lozano-Vila, A. M.; Monsaert, S.; Bajek, A.; Verpoort, F. *Chem. Rev.* **2010**, *110*, 4865−4909.
(7) Samojlowicz, C.; Bieniek, M.; Grela, K. *Chem. Rev.* **2009**, *109*, 3708−3742.
(8) Alcaide, B.; Almedros, P.; Luna, A. *Chem. Rev.* **2009**, *109*, 3817−3858.
(9) Conley, B. L.; Pennington-Boggio, M. K.; Boz, E.; Williams, T. J. *Chem. Rev.* **2010**, *110*, 2294−2312.
(10) Guo, X.; Li, C.-J. *Org. Lett.* **2011**, *13*, 4977−4979.
(11) Juliá-Hernández, F.; Simonetti, M.; Larosa, I. *Angew. Chem., Int. Ed.* **2013**, *52*, 11458−11460.
(12) Astruc, D. *New. J. Chem.* **2005**, *29*, 42−56.
(13) Harmon, R. E.; Gupta, S. K.; Brown, D. J. *Chem. Rev.* **1973**, *73*, 21−52.
(14) (a) Bianchini, C.; Meli, A.; Peruzzini, M.; Vizza, F.; Zanobini, F. *Coord. Chem. Rev.* **1992**, *120*, 193−208. (b) Mayer, H. A.; Kaska, W. C. *Chem. Rev.* **1994**, *94*, 1239−1272. (c) Hierso, J.-C.; Amardeil, R.; Bentabet, E.; Broussier, R.; Gautheron, B.; Meunier, P.; Kalck, P. *Coord. Chem. Rev.* **2003**, *236*, 143−206.
(15) (a) MacBeth, C. E.; Harkins, S. B.; Peters, J. C. *Can. J. Chem.* **2005**, *83*, 332−340. (b) Fernández-Anca, D.; García-Seijo, M. I.; García-Fernández, M. E. *Dalton Trans.* **2010**, *39*, 2327−2336. (c) Lipke, M. C.; Tilley, T. D. *Angew. Chem., Int. Ed.* **2012**, *51*, 11115−11121.
(16) (a) Bianchini, C.; Frediani, M.; Vizza, F. *Chem. Commun.* **2001**, 479−480. (b) Chr. van Engele, M.; Teunissen, H. T.; de Vries, J. G.; Elsevier, C. J. *J. Mol. Catal. A: Chem.* **2003**, *206*, 185−192. (c) Chaplin, A. B.; Dyson, P. J. *Inorg. Chem.* **2008**, *47*, 381−390. (d) Rosales, M.; Vallejo, R.; Soto, J. J.; Bastidas, L. J.; Molina, K.; Baricelli, P. J. *Catal. Lett.* **2010**, *134*, 56−62. (e) Rosi, L.; Frediani, M.; Frediani, P. *J. Organomet. Chem.* **2010**, *695*, 1314−1322. (f) Sarmah, B. J.; Dutta, D. K. *J. Organomet. Chem.* **2010**, *695*, 781−785. (g) Chaplin, A. B.; Dyson, P. J. *J. Organomet. Chem.* **2011**, *696*, 2485−2490. (h) Coetzee, J.; Dodds, D. L.; Klankermayer, J.; Brosinski, S.; Leitner, W.; Slawin, A. M. Z.; Cole-Hamilton, D. J. *Chem. Eur. J.* **2013**, *19*, 11039−11050.
(17) Miller, P. W.; White, A. J. P. *J. Organomet. Chem.* **2010**, *695*, 1138−1145.
(18) (a) Kyran, S. J.; Muhammad, S.; Knestrick, M.; Bengali, A. A.; Darensbourg, D. J. *Organometallics* **2012**, *31*, 3163−3170. (b) Schober, P.; Soltek, R.; Huttner, G.; Zsolnai, L.; Heinze, K. *Eur. J. Inorg. Chem.* **1998**, 1407−1415.
(19) Alidori, S.; Heift, D.; Santiso-Quinones, G.; Benkö, Z.; Grützmacher, H.; Caporali, M.; Gonsalvi, L.; Rossin, A.; Peruzzini, M. *Chem. Eur. J.* **2012**, *18*, 14805−14811.
(20) Siegl, W. O.; Lapporte, S. J.; Collman, J. P. *Inorg. Chem.* **1973**, *12*, 674−677.
(21) Bianchini, C.; Meli, A.; Laschi, F.; Ramirez, J. A.; Zanello, P.; Vacca, A. *Inorg. Chem.* **1988**, *27*, 4429−4435.
(22) Bianchini, C.; Meli, A.; Peruzzini, M.; Vizza, F.; Fujiwara, Y.; Jintoku, T.; Taniguchi, H. *J. Chem. Soc., Chem. Commun.* **1988**, 299−301.
(23) Bianchini, C.; Barbaro, P.; Macchi, M.; Meli, A.; Vizza, F. *Helv. Chim. Acta* **2001**, *84*, 2895−2923.
(24) Söncksen, L.; Gradert, C.; Krahmer, J.; Näther, C.; Tuczek, F. *Inorg. Chem.* **2013**, *52*, 6576−6589.
(25) Mellone, I.; Peruzzini, M.; Rosi, L.; Mellmann, D.; Junge, H.; Beller, M.; Gonsalvi, L. *Dalton Trans.* **2013**, *42*, 2495−2051.
(26) Beydoun, K.; vom Stein, T.; Klankermayer, J.; Leitner, W. *Angew. Chem., Int. Ed.* **2013**, *52*, 9554−9557.
(27) Geilen, F. M. A.; Engendahl, B.; Harwardt, A.; Marquardt, W.; Klankermayer, J.; Leitner, W. *Angew. Chem., Int. Ed.* **2010**, *49*, 5510−5514.
(28) Aycock, D. F. *Org. Process Res. Dev.* **2007**, *11*, 156−159.
(29) Milton, E. J.; Clarke, M. L. *Green Chem.* **2010**, *12*, 381−383.
(30) Green Chemistry Highlights. *Org. Process Res. Dev.* **2011**, *15*, 22−30.
(31) Vom Stein, T.; Weigand, T.; Merkens, C.; Klankermayer, J.; Leitner, W. *ChemCatChem* **2012**, *5*, 439−441.
(32) Wesselbaum, S.; vom Stein, T.; Klankermayer, J.; Leitner, W. *Angew. Chem., Int. Ed.* **2012**, *51*, 7499−7502.
(33) Märkl, G.; Jin, G. Y. *Tetrahedron Lett.* **1981**, *22*, 1105−1108.
(34) Fillol, J. L.; Kruckenberg, A.; Scherl, P.; Wadepohl, H.; Gade, L. H. *Chem. Eur. J.* **2011**, *17*, 14047−14062.
(35) Rodríguez, L.-I.; Roth, T.; Fillol, J. L.; Wadepohl, H.; Gade, L. H. *Chem. Eur. J.* **2012**, *18*, 3721−3728.
(36) Scherl, P.; Kruckenberg, A.; Mader, S.; Wadepohl, H.; Gade, L. H. *Organometallics* **2012**, *31*, 7024−7027.
(37) Scherl, P.; Wadepohl, H.; Gade, L. H. *Organometallics* **2013**, *32*, 4409−4415.
(38) van der Boom, M. E.; Milstein, D. *Chem. Rev.* **2003**, *103*, 1759−1792.
(39) Choi, J.; MacArthur, A. H. R.; Brookhart, M.; Goldman, A. S. *Chem. Rev.* **2011**, *111*, 1761−1779.
(40) Selander, N.; Szabó, K. J. *Chem. Rev.* **2011**, *111*, 2048−2076.
(41) Salem, H.; Shimon, L. J. W.; Diskin-Posner, Y.; Leitus, G.; Ben-David, Y.; Milstein, D. *Organometallics* **2009**, *28*, 4791−4806.
(42) Fogler, E.; Balaraman, E.; Ben-David, Y.; Leitus, G.; Shimon, L. J. W.; Milstein, D. *Organometallics* **2011**, *30*, 3826−3833.
(43) Balaraman, E.; Fogler, E.; Milstein, D. *Chem. Commun.* **2012**, *48*, 1111−1113.
(44) Srimani, D.; Feller, M.; Ben-David, Y.; Milstein, D. *Chem. Commun.* **2012**, *48*, 11853−11855.
(45) Srimani, D.; Ben-David, Y.; Milstein, D. *Angew. Chem., Int. Ed.* **2013**, *52*, 4012−4015.
(46) Hölscher, M.; Prechtl, M. H. G.; Leitner, W. *Chem. Eur. J.* **2007**, *13*, 6636−6643.
(47) Alós, J.; Bolaño, T.; Esteruelas, M. A.; Oliván, M.; Oñate, E.; Valencia, M. *Inorg. Chem.* **2014**, *53*, 1195−1209.
(48) Hanton, M. J.; Tin, S.; Boardman, B. J.; Miller, P. *J. Mol. Catal. A: Chem.* **2011**, *346*, 70−78.
(49) Cavit, B. E.; Grundy, K. R.; Roper, W. R. *J. Chem. Soc., Chem. Commun.* **1972**, 60−61.
(50) Letts, J. B.; Mazanec, T. J.; Meek, D. *Organometallics* **1983**, *2*, 695−704.
(51) Nakamoto, K. *Infrared and Raman Spectra of Inorganic and Coordination Compounds Part B: Applications in Coordination, Organometallic, and Bioinorganic Chemistry*; Wiley-Interscience: Hoboken, NJ, 2009.
(52) Geilen, F. M. A.; Engendahl, B.; Hölscher, M.; Klankermayer, J.; Leitner, W. *J. Am. Chem. Soc.* **2011**, *133*, 14349−14358.
(53) Rhodes, L. F.; Venanzi, L. M. *Inorg. Chem.* **1987**, *26*, 2692−2695.
(54) Bakhmutov, V. I.; Bakmutova, E. V.; Belkova, N. V.; Bianchini, C.; Epstein, L. M.; Masi, D.; Peruzini, M.; Shubina, E. S.; Voronstov, E. V.; Zanobini, F. *Can. J. Chem.* **2001**, *79*, 479−489.
(55) Rappert, T.; Yamamoto, A. *Organometallics* **1994**, *13*, 4984−4993.